



ISSN: 2350-0328

**International Journal of Advanced Research in Science,
Engineering and Technology**

Vol. 4, Issue 8 , August 2017

Application of Adaptive Particle Swarm Optimization Algorithm in Prestressed Concrete Bridge Design

Mohsen Maniat, Masoud Arab-Naeini, Hosein Naderpour ,Ali Kheyroddin

Graduate Student, Department of Civil Engineering, The University of Memphis, Memphis, TN 38152, USA
Graduate Student, Department of Civil Engineering, Semnan University, Semnan, Iran
Associate Professor, Department of Civil Engineering, Semnan University, Semnan, Iran
Professor, Department of Civil Engineering, Semnan University, Semnan, Iran

ABSTRACT:The purpose of this paper is to optimize post-tensioned concrete box girder bridge superstructures. Several variables are considered including cross-sectional dimensions of the girder, concrete strength, prestressing force, number of tendons, number of strands per tendon, tendons arrangement, and reinforcements of slabs. AASHTO Standard Specifications for Highway Bridges is considered for the purpose of loading, analyzing, and designing. The objective function consists of material and construction costs of concrete, prestressing steel, reinforcement, and formwork. A Particle Swarm Optimization (PSO) algorithm with adaptive inertia weight is developed to minimize the total cost of the bridges in a short time. Since constant design parameters influence the optimum design, a parametric study is conducted for different values of span length and deck width of the bridge. A comparison between the results obtained by a Genetic Algorithm (GA) and the PSO algorithm is conducted to show the efficiency of the proposed algorithm.

KEYWORDS: Particle Swarm Optimization, Structural Optimization, Bridge Optimization, Prestressed Concrete Bridge, Post-Tensioning, Metaheuristic Algorithms.

I.INTRODUCTION

Because of their durability and economy of construction, prestressed concrete bridges are very common. Post-tensioned concrete box girders are popular among these bridges. In addition, single box arrangements are efficient for both longitudinal and transverse designs, and they may be counted as an economic solution for most medium and long span bridges [1]. As several variables are involved in designing of these types of bridges, a wide variety of designs are possible for a bridge with certain span length and deck width. In the traditional design method, designers use a trial and error process along with their experience resulting in a high cost, time, and human effort. The optimization techniques change the process of trial and error to a systematic and computer-based procedure that yields an optimum design in term of given criteria such as weight or cost, while considering all functional purposes of the design.

During the past decades, considerable research has been conducted on optimization of different structures. Most of these studies are focused on weight minimization [2-5]. While weight of a structure constitutes a significant part of the cost, a minimum weight design is not necessarily the minimum cost design [6]. Since different materials including concrete and steel are involved in construction of concrete structures, optimization of these structures should be based on cost rather than weight [7].

In prestressed concrete design optimization, the problem is nonlinear requiring the use of nonlinear optimization procedures [8]. Early works on optimization of these structures have linearized the nonlinear problem [9-12]. A review of cost optimization of concrete and steel structures is presented by Adeli and Sarma[6]. Cost optimization of post-tensioned prestressed concrete T-section beams was presented by Goble and Lapay[13] using gradient projection method. Kirsch [14] studied the minimum cost design of continuous prestressed concrete beams and solved it by the linear programming (LP) method. Naaman [15] compared minimum cost designs with minimum weight designs for prestressed rectangular beams and one-way slabs by using a direct search technique. Cohn and MacRae[16] presented the cost optimum design of simply supported RC and partially or fully pre-tensioned and post-tensioned concrete beams of fixed cross-sectional geometry using the feasible conjugate-direction method. Jones [17] minimized the cost



of precast, prestressed concrete simply supported box girders used in a multi-beam highway bridge using integer programming method. Cohn and Lounis[18] presented the cost optimization of partially and fully prestressed concrete continuous beams and one-way slabs based on the limit state design and projected Lagrangian algorithm. Torres et al. [19] optimized the cost of prestressed concrete highway bridges by using a linear programming method. Using general geometric programming, Yu et al. [20] presented the cost optimum design of a prestressed concrete box girder bridge. The previous procedure was also used by Barr et al. [21] to optimize the cost of a continuous three-span bridge RC slab. Lounis and Cohn [22] studied the cost minimization of highway bridges consisting of RC slabs on precast, post-tensioned concrete I-girders using a three-level optimization approach. Further studies on cost optimization of bridges have been done by Lounis and Cohn [23-25]. Fereig[26] presented the minimum cost preliminary design of single span bridges consisting of cast-in-place RC deck and girders. The author linearized the nonlinear problem and solved it by the Simplex method. Sirca and Adeli[27] presented an optimization method to minimize the cost of the pretensioned PC I-beam bridge system. The nonlinear programming problem was solved by using a patented robust neural dynamics model. Ayvaz and Aydin [28] minimized the cost of a pretensioned PC I-girder bridge using a genetic algorithm by considering 9 different variables and a total of 28 constraints. Ahsan et al. [29] presented the cost optimum design of post-tensioned I-girder bridges by considering 14 different variables, 28 explicit constraints, and 46 implicit constraints using an evolutionary operation (EVOP). Kaveh et al. [30] proposed a modified colliding bodies optimization algorithm to minimize the cost of the post-tensioned concrete bridges. Abbasi et al. [31-34] carried out an extensive study about seismic behavior of post-tensioned reinforced concrete bridges with different configurations including, straight, skewed, and curved with equal and unequal pier heights.

In this study, cost optimum design of post-tensioned concrete box girder bridge superstructures is presented. The cost objective function includes the material and construction costs of concrete, prestressing steel, reinforcement, and formwork. Concrete strength is taken a design variable, so unit cost of concrete is assumed a function of concrete strength. AASHTO Standard Specifications for Highway Bridges [35] is used for analysis and design the bridge superstructure in both longitudinal and transverse directions. Instead of using a lumped sum value, all instantaneous and long-term prestress losses are calculated based on AASHTO formulas. Particle Swarm Optimization with adaptive inertia weight has been used in this paper to solve the optimization problem. A comparison between the optimum results of the PSO and the genetic algorithm is presented. Finally, as constant design parameters influence the optimum design, a parametric study is carried out for different values of constant parameters.

II. PROBLEM FORMULATION

The cast-in-place post-tensioned concrete box girder bridge which is simply supported is assumed to be constructed using span-by-span method. In defining the optimization problem, 17 different variables, 34 explicit constraints, and 106 implicit constraints are considered which are introduced in the subsequent sections.

A) Design variables and constant parameters

The variables considered in this study are concrete strength, cross-sectional dimensions of the box girder, number of strands per tendon, number of tendons in each web, arrangement of tendons, prestressing force, and reinforcements of slabs. Since concrete strength is considered a design variable, modulus of elasticity of concrete is a function of concrete strength. Design variables are tabulated in Table 1, and a typical cross-section of the assumed bridge with some of the variables is shown in Figure 1. The constant design parameters considered in this study are span length, deck width, post-tensioning anchorage system, AASHTO live loads, superimposed dead loads, and properties of the materials except concrete strength. 15 mm diameter seven-wire low relaxation strands are used for tendons, and the Freyssinet C-range anchorage system is used for post-tensioning the tendons [36]. The constant design parameters are shown in Table 2.

Configuration of tendons significantly affects flexural stresses and prestress losses at different sections. Number of strands per tendon, number of tendons, number of anchorages in each row, and lowest anchorage position are defined as variables to cover various tendons configuration. Longitudinal profiles of tendons along the span vary as parabolic curve in the webs of the girder. As shown in Figure 2, in addition to cross-sectional dimensions, configuration of tendons at the end and middle sections depends on different parameters including duct size, anchorage spacing, and

anchorage edge distances. According to Freyssinet post-tensioning system, these parameters are function of number of strands per tendon which is assumed as a design variable in this study. Anchorage spacing and anchorage edge distance are also function of concrete strength, and minimum vertical anchorage distance to bottom fiber is related to jack dimension. These parameters for a concrete strength of 40 MPa are shown in Table 3.

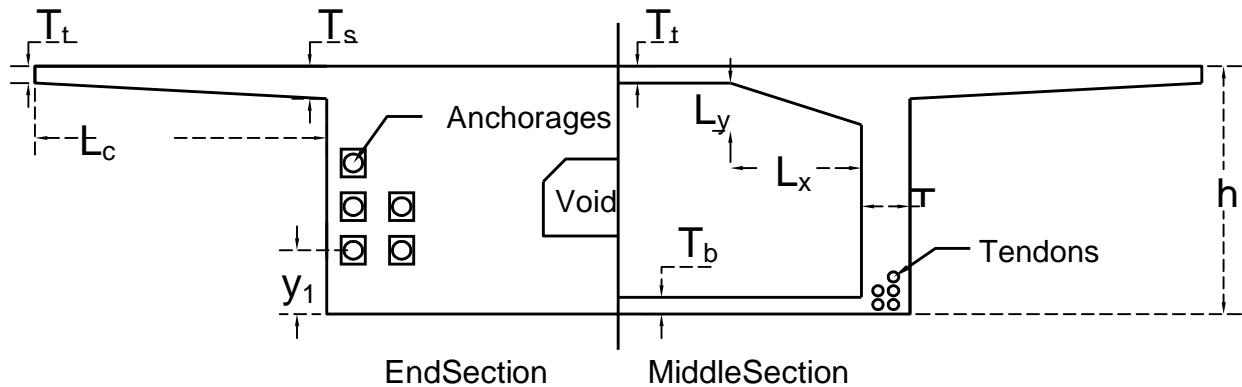


Fig. 1. Box girder cross-section.

Table 1. Design variables and explicit constraints.

No.	Variable	Explicit constraint
1	Concrete strength, f'_c (MPa)	$35 \leq f'_c \leq 50$
2	Girder depth, h (m)	$1.5 \leq h \leq 4$
3	Top slab thickness, T_t (cm)	$17.5 \leq T_t \leq 35$
4	Bottom slab thickness, T_b (cm)	$17.5 \leq T_b \leq 30$
5	Web thickness, T_w (cm)	$25 \leq T_w \leq 50$
6	Length of cantilever, L_c (m)	$1 \leq L_c \leq 1/4W$
7	End thickness of cantilever, T_c (cm)	$17.5 \leq T_c \leq 30$
8	Initial thickness of cantilever, T_s (cm)	$20 \leq T_s \leq 50$
9	Length of haunch, L_x (cm)	$50 \leq L_x \leq 200$
10	width of haunch, L_y (cm)	$25 \leq L_y \leq 50$
11	Number of strands per tendon, N_s	$5 \leq N_s \leq 25$
12	Number of tendons in each web, $N_f/2$	$1 \leq N_f/2 \leq 10$
13	Number of anchorages in each row, N_A	1 or 2
14	Lowest anchorage position, y_1 (cm)	$y_{min} \leq y_1 \leq 100$
15	Prestressing force, η (% of f_y^*)	$0.75\% \leq \eta \leq 0.90\%$
16	Top slab reinforcement ratio, ρ_s	$\rho_{min} \leq \rho_s \leq \rho_{max}$
17	Cantilever slab reinforcement ratio, ρ_c	$\rho_{min} \leq \rho_c \leq \rho_{max}$

Table 2. Constant design parameters.

Constant parameter	Value
Span length (L)	30,40,50,and 60 m
Deck width (W)	8,10,12,and 14 m
Concrete strength at transfer (f'_{ci})	$0.7 f'_c$
Tensile strength of prestressing steel (f_{pu})	1860 MPa
Yield strength of prestressing steel (f_y^*)	$0.9 f_{pu}$
Yield strength of reinforcement steel (f_y)	400 MPa
Unit weight of concrete	2400 kg/m ³
Unit weight of Steel	7850 kg/m ³
Modulus of elasticity (E) of concrete	$5 \sqrt{f'_c}$ GPa
E of prestressing steel	193 GPa
E of reinforcement steel	200 GPa
Wobble coefficient (K)	0.00066 /m
Friction coefficient (μ)	0.25
Anchor set	5 mm
Live loads	HS20-44
Design traffic lane width	3.65 m
Barrier width	45 cm
Barrier load	500 kg/m
Thickness of asphalt wearing surface	8 cm
Unit weight of asphalt wearing surface	1730 kg/m ³
Thickness of end diaphragms	80 cm
Relative humidity (RH)	50%
Manhole Length	1.6 m
Manhole Width	1 m

Table 3. Minimum dimensions for Freyssinet C-range anchorage system (mm) for $f'_c=40$ MPa.

Number of strands per tendon (N_s)	5-7	8-9	10-12	13	14-19	20-22	23-25
Duct size (D)	65	70	85	85	100	110	115
Horizontal anchorage spacing (x)	370	422	472	503	587	649	690
Vertical anchorage spacing (y)	267	305	341	364	424	469	498
Horizontal anchorage edge distance (x_e)	213	239	264	280	322	352	373
Vertical anchorage edge distance (y_e)	162	181	199	210	240	262	277
Minimum anchorage distance to bottom fiber (y_{min})	230	230	230	230	269	347	347

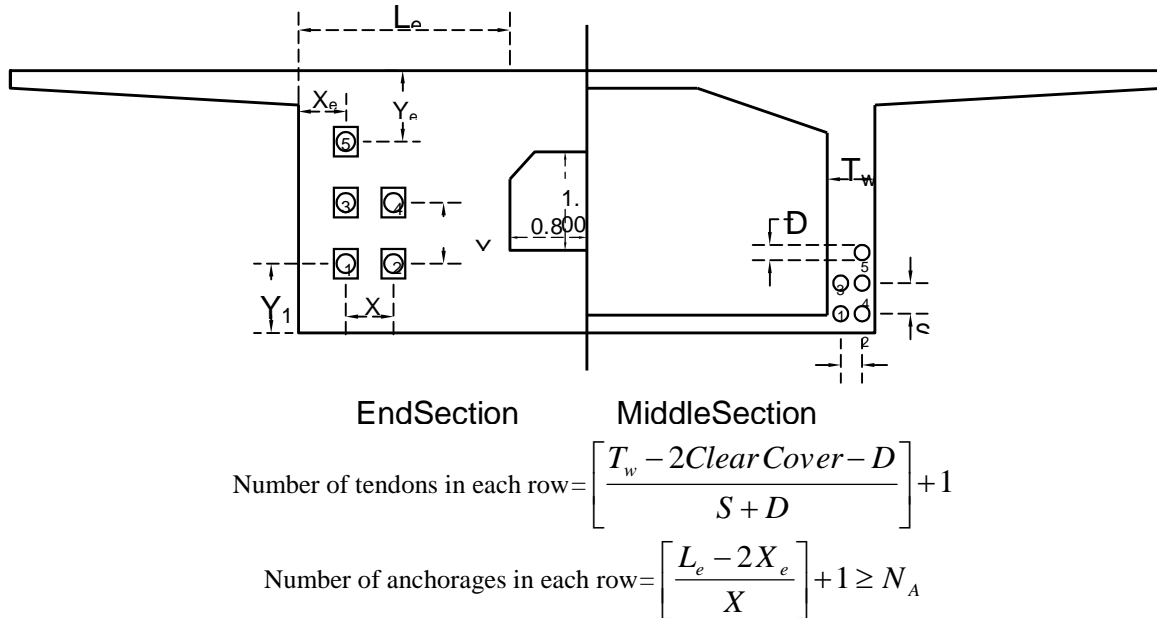


Fig.2..Tendons arrangement at the end and middle sections.

B) Objective function

The goal of the optimization problem is to minimize the cost of the bridge superstructures. Material and construction costs of concrete, prestressing steel, reinforcement, and formwork are considered in the objective function as follows:

$$C_T = \frac{V_c \cdot C_c + W_{ps} \cdot C_{ps} + W_r \cdot C_r + A_f \cdot C_f}{W.L} \quad (1)$$

Where C_T is the total cost of the box girder per square meter of the deck. V_c , W_{ps} , W_r , and A_f are volume of concrete, weight of prestressing steel, weight of reinforcements, and surface area of formwork, respectively. C_c , C_{ps} , C_r , and C_f are unit material and construction costs of concrete, prestressing steel, reinforcement, and formwork, respectively.

The unit costs of different materials are shown in Table 4. Analysing the prices of concrete with different strengths, a linear function is estimated for unit cost of concrete. In calculation of weight of reinforcement steel, all reinforcements including shrinkage and temperature, computational tensile, distribution, and shear reinforcements are taken into account.

C) Explicit constraints

Explicit constraints are lower and upper bounds of the design variables based on geometrical restraints, construction limitations, and code requirements. In Table 1, all of the explicit constraints considered in this paper are summarized. Lower limit of concrete strength (f_c) is assumed 35 MPa since, according to Freyssinet, minimum concrete strength at transfer (f_{ci}) is 24 MPa ($f_{ci} = 0.7f_c$). Because of practical restrictions, concrete strength is assumed no greater than 50 MPa. Minimum depth of the girder is 1.5 m to resist flexural and shear stresses, and its maximum is 4 m from the aesthetic point of view. The top slab thickness has a lower limit of 17.5 cm to accommodate reinforcements and to transfer truck wheel load, and has an upper limit of 35 cm. The minimum web thickness is 25 cm to facilitate concreting and consolidating, and the maximum value is assumed 50 cm to avoid a too heavy bridge. The maximum length of cantilever is one-fourth of the bridge width, and the minimum is set to 1 m. It is assumed that the number of strands per tendon varies from 5 to 25. The prestressing force is applied as a percentage of yield strength of prestressing steel (f_y^*). For this study, the prestressing force is considered no less than $0.75f_y^*$ for efficient use of prestressing steel, and the upper bound is $0.9f_y^*$ according to AASHTO.

D)Implicit constraints

These constraints are formulated according to AASHTO standard specifications to control the performance requirements of the bridge. The superstructure is designed in both longitudinal and transverse directions; in longitudinal direction, we deal with a prestressed concrete design, and in transverse direction, with a reinforced concrete design. The total 106 implicit constraints in this study is are categorized into 8 groups, and are explained in the following.

- *Flexural working stress constraints*

Stresses in the top and bottom fibers of concrete should not exceed the allowable tensile and compressive stresses. The related implicit constraints are defined as follows:

$$\sigma_c \leq \sigma \leq \sigma_t \quad (2)$$

$$\sigma = \frac{F}{A} + \frac{F \cdot e}{S} + \frac{M}{S} \quad (3)$$

Where σ , σ_c , and σ_t are working stress, allowable compressive stress, and allowable tensile stress respectively; F is prestressing force ; A is cross-sectional area of the girder; e is tendons eccentricity; M is working moment; and S is section modulus.

Allowable stresses are controlled for 4 load conditions (Table 5) and in 5 critical sections along the girder span (Figure 3). Section at midspan (section 1); section after the anchor set (section 2); section at the end of transition zone assumed $1.5h$ (section 3); section immediately after the diaphragm assumed $0.8 m$ (section 4); end section (section 5).

Table 4. Unit costs of materials.

Item	unit	Unit cost
C_c	per m^3	\$ $0.59 f'_c + 17.91$
C_{ps}	per ton	\$ 3000
C_r	per ton	\$ 636
C_f	per m^2	\$ 7.12

f'_c : 28-day compressive concrete strength (MPa)

Table 5. Different load conditions and related implicit constraints.

No.	Working Stress	Implicit Constraint
1	$\sigma = \frac{F_i}{A} + \frac{F_i \cdot e}{S} + \frac{M_D}{S}$	$-0.55 f'_{ci} \leq \sigma \leq 0.009 \sqrt{f'_{ci}} \text{ (MPa)}$
2	$\sigma = \frac{F_e}{A} + \frac{F_e \cdot e}{S} + \frac{M_D + M_{Sl}}{S}$	$-0.40 f'_c \leq \sigma \leq 0.019 \sqrt{f'_c} \text{ (MPa)}$
3	$\sigma = \frac{F_e}{A} + \frac{F_e \cdot e}{S} + \frac{M_D + M_{Sl} + M_L}{S}$	$-0.60 f'_c \leq \sigma \leq 0.019 \sqrt{f'_c} \text{ (MPa)}$
4	$\sigma = \frac{0.5 F_e}{A} + \frac{0.5 F_e \cdot e}{S} + \frac{0.5 (M_D + M_{Sl}) + M_L}{S}$	$-0.40 f'_c \leq \sigma \leq 0.019 \sqrt{f'_c} \text{ (MPa)}$

Note: F_i =prestressing force after instantaneous losses; F_e = prestressing force after all losses; M_D , M_{Sl} and M_L =working moments of dead, superimposed and live loads.

Since prestress losses are functions of the design variables, all prestress losses are calculated according to AASHTO formulas rather than using estimates of total losses for greater precision. Prestress losses are categorized into two groups; instantaneous losses and long-term losses. Instantaneous losses which occur during prestressing the tendons and transferring the prestress force to the concrete member are including friction loss, elastic shortening loss, and anchorage seating loss. Long-term losses which occur during the service life of the member are losses due to concrete shrinkage, creep of concrete, and relaxation of prestressing steel.

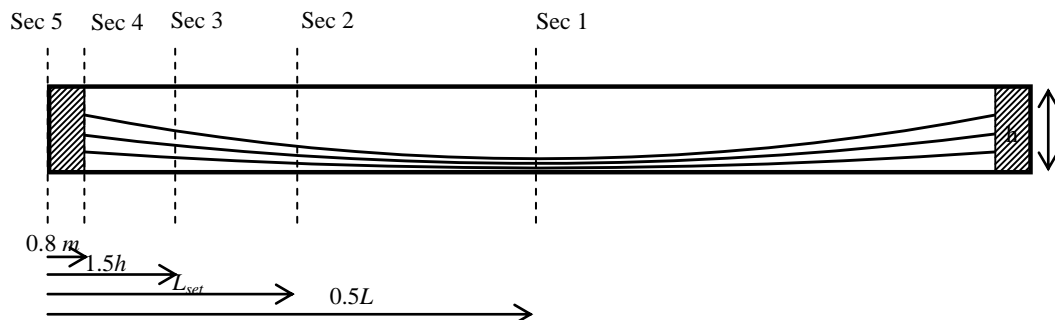


Fig. 3. Critical sections along the span and the profile of the tendons.

- *Allowable stress in prestressing steel constraints*

These constraints control tensile stresses in the pressing steel. According to AASHTO, allowable stress in prestressing steel immediately after seating at anchorage is $0.7f_{pu}$, at the end of the seating loss zone is $0.83f_y^*$, and at service load after all losses is $0.80f_y^*$. The related implicit constraints are as follows:

$$(1-1) \quad \frac{F_{5i}}{A_s} \leq 0.7 f_{pu} \quad (4)$$

$$(1-2) \quad \frac{F_{2i}}{A_s} \leq 0.83 f_y^* \quad (5)$$

$$(1-3) \quad \frac{F_{2e}}{A_s} \leq 0.80 f_y^* \quad (6)$$

Where F_{5i} and F_{2i} are prestressing forces at sections 5 and 2 after instantaneous losses, respectively. F_{2e} is prestressing force at section 2 after long-term losses, and A_s is the total area of prestressing steel.

- *Ultimate flexural strength constraints*

The flexural strength of the girder is controlled at four different sections (section 1 to 4). These constraints are based on the Ultimate Strength Design (USD) method and are as follows:

$$(1-4) \quad M_u \leq \phi M_n \quad (7)$$

Where M_u is factored bending moments at different sections, and ϕM_n is flexural strength of the section which ϕ is strength reduction factor for flexure.

- *Ductility constraints*

The total amount of prestressing steel should be adequate to develop an ultimate moment at the critical section at least 1.2 times the cracking moment M_{cr}^* . The minimum prestressing steel constraints are considered at sections 1 to 4 and are as follows:

$$(1-5) \quad 1.2M_{cr}^* \leq \phi M_n \quad (8)$$

Where M_{cr}^* and ϕM_n are cracking moment and ultimate moment, respectively. AASHTO states that prestressed concrete members shall be designed so that the steel is yielding as the ultimate capacity is approached. To meet this requirement, the reinforcement index shall not exceed $0.36\beta_1$. The maximum prestressing steel constraints are considered at sections 1 to 4, and are as follows, where ω is reinforcement index, and β_1 is a concrete strength factor.

$$(1-6) \quad \omega \leq 0.36\beta_1 \quad (9)$$

- *Ultimate shear strength constraints*

The shear strength of the girder is controlled at four different sections (section 1 to 4). The section at $0.25h$ is also checked to compute shear reinforcement. These constraints are as follows, Where V_u , V_c , and V_s are factored shear force at different sections, nominal shear strengths provided by concrete, and shear reinforcement, respectively. ϕ is strength reduction factor for shear.

$$(1-7) \quad V_u \leq \phi(V_c + V_s) \quad (10)$$

- *Deflection constraint*

The long-term deflection of the box girder is calculated in midspan, and is limited as follows, where Δ is deflection in midspan, and L is the span length.

$$(1-8) \quad \Delta \leq \frac{L}{800} \quad (11)$$

- *Slab design constraints*

Three slabs including top, bottom, and cantilever slabs are designed based on ultimate strength design method. The related implicit constraints are the same as Equation (7).

- *Cantilever slab deflection constraint*

Deflection of cantilever slab is limited as follows:

$$(1-9) \quad \Delta \leq \frac{L_c}{300} \quad (12)$$

Where Δ is deflection at the end of the cantilever, and L_c is the length of cantilever.

E) The optimization problem

The optimization problem is determined by 17 variables, 34 explicit constraints, 106 implicit constraints, and a cost objective function explained in the preceding sections. The objective function and most of the implicit constraints are nonlinear functions of the design variables requiring the use of nonlinear optimization procedures. During the past several decades, many mathematical linear and nonlinear programming methods have been developed for solving optimization problems. Some of these methods search for a local optimum by moving in a direction related to the local gradient. Other methods apply the first and second-order necessary conditions to seek a local minimum by solving a set of nonlinear equations. For the optimum design of large structures, these methods become inefficient due to a large amount of gradient calculations [6]. Therefore, an advance optimization technique is required to locate the global minimum in a short time without being entrapped in local minima.

III. PARTICLE SWARM OPTIMIZATION

Particle swarm optimization (PSO) is a simple and effective algorithm for optimizing a wide range of functions. Conceptually, the PSO seems to lie somewhere between Genetic Algorithm (GA) and evolutionary programming [37]. The PSO utilizes the real-number and the global communication among the swarm particles. Therefore, it is easier to handle in comparison with GAs as there is no need to encode or decode the parameters into binary strings [38]. The algorithm contains number of particles, each which is a possible solution for the objective function. Particles are initialized randomly in the search space. In each iteration, the velocities of particles are updated by means of their best encountered positions, and the best position encountered by the particles using the following formula [39 and 40]:

$$(1-10) \quad v_i^{k+1} = \rho_i^k v_i^k + C_1 r_1 (P_i^k - X_i^k) + C_2 r_2 (P_g^k - X_i^k) \quad (13)$$

Where P_i^k (personal best) is the best previous position of the i th particle in the k th iteration, and P_g^k (global best) is the best global position among all the particles in the swarm in the k th iteration. r_1 and r_2 are random values, uniformly distributed between zero and one. C_1 and C_2 are the cognitive and social scaling parameters, respectively, and ρ_i^k is the inertia weight used to discount the previous velocity of the particle. The position of each particle is updated in each iteration by adding the velocity vector to the position vector as:

$$X_i^{k+1} = X_i^k + v_i^{k+1} \quad (14)$$

Where X_i^k and v_i^{k+1} represent the current position and velocity vectors of the i th particle, respectively. Velocity vectors v_i are limited to a lower bound v_{min} and an upper bound v_{max} . Different techniques have been used to set some of the PSO parameters, such as fuzzy systems [41], self-adaptation [42] and deterministic adaptation based on personal and global bests [43]. Ratnaweera et al. [44] proposed a time-varying acceleration coefficient (TVAC), which reduces the cognitive component and increases the social component of acceleration coefficient with time. A large value of C_1 and a small value of C_2 at the beginning may improve the exploration ability, and a small value of C_1 and a large value of C_2 allow the particles converge to the global optimum in the later part of the optimization. A nonlinear function is used to calculate C_1 and C_2 according to the following equations:

$$C_1 = C_{max} - [(C_{max} - C_{min}) \times \frac{iter}{iter_{max}}]^n \tag{15}$$

$$C_2 = C_{max} + [(C_{max} - C_{min}) \times \frac{iter}{iter_{max}}]^m \tag{16}$$

Where C_{min} and C_{max} are the lower and upper bounds for both C_1 and C_2 . Here, $iter$ is the current iteration number and $iter_{max}$ is the maximum number of allowable iterations. According to the type of the problem, n and m can be chosen to get more efficient results. In this paper, n and m are taken to 1 and 2 respectively, also C_{min} and C_{max} are chosen 2.4 and 2.7, respectively. The velocities of all the particles are limited to the range specified by v_{min} and v_{max} which are equal to $\pm (X_{min} - X_{max})/4$. An adaptive strategy based on the ranks of particles in each iteration has been used in order to define inertia weight [45].

$$\rho_i^k = \rho_{min} + (\rho_{max} - \rho_{min}) \times \frac{rank_i}{number\ of\ particles} \tag{17}$$

Where ρ_{min} and ρ_{max} are the lower and upper bounds of inertia weight. $rank_i$ is the position of the i th particle when the particles are sorted based on their fitness values. The rationale behind this formula is that the positions of the particles are adjusted in a way that the best particles move more slowly compared to the worst ones [46]. The flowchart of the algorithm is shown in Figure 4.

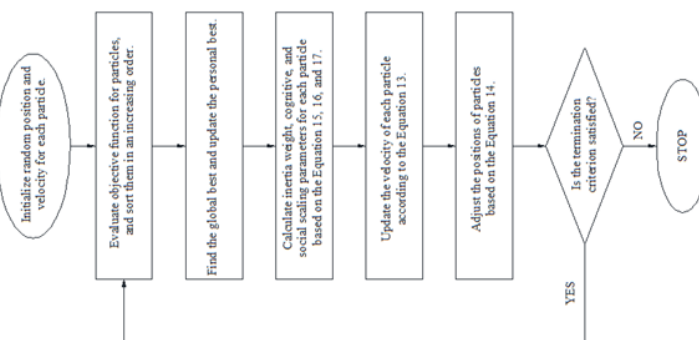


Fig. 4. The flowchart of adaptive PSO algorithm.

IV. OPTIMIZATION RESULTS

In this section, several bridges with different span lengths and deck widths are optimized using the proposed PSO algorithm and a comparison between the performance of PSO and GA is conducted. The whole analysis and design process is conducted automatically and only the size and number of rebars are manually selected based on the required steel amount. The cross-section of the optimum design of a bridge with the span length of 50 m and the deck width of 12 m and its shear reinforcements along the girder span for half of the span are shown in Figure 5 and 6. As seen in the figures, the girder depth is 3.21 m which accommodates anchorages in one column, and the thick webs provided adequate space to place two tendons in each row. Web thickness and initial thickness of cantilever stick to their upper limits. In addition, a total 168 prestressing seven-wire strands are used for the whole section.

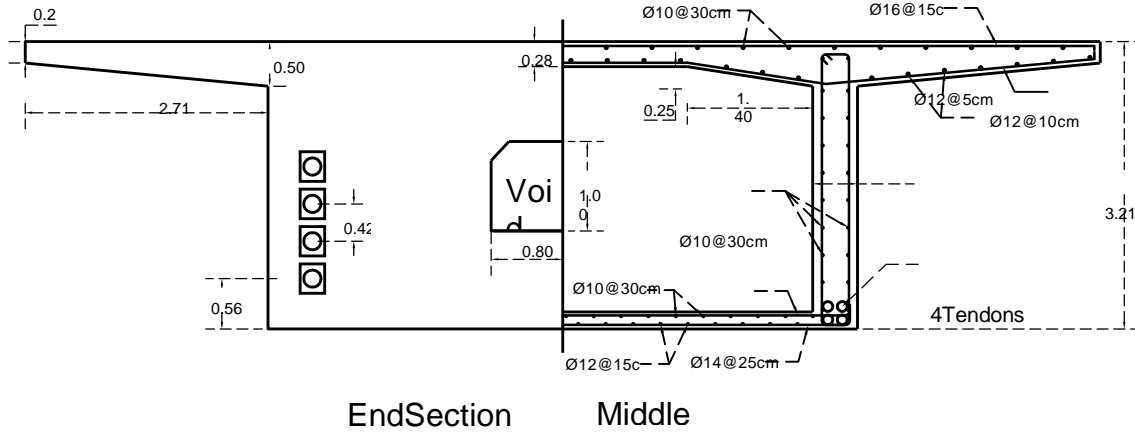


Fig. 5 Optimum post-tensioned concrete box girder bridge cross-section.

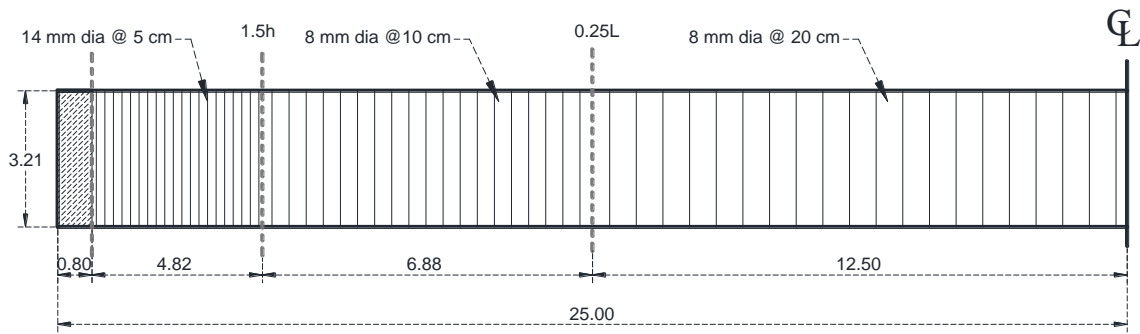


Fig. 6. Shear reinforcements of the optimum design.

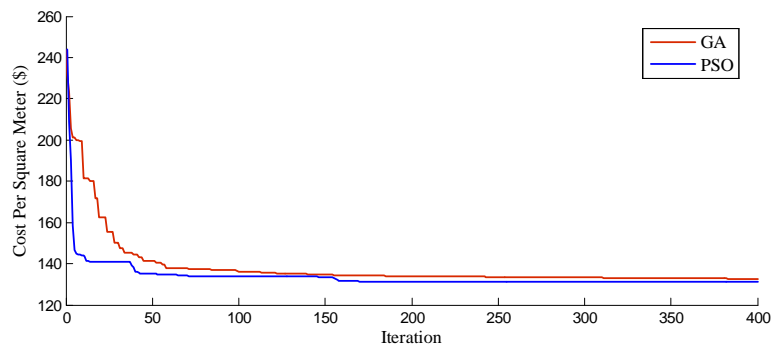


Fig. 7. The convergence history of the PSO and GA.

Since the constant design parameters influence the optimum design, this optimization is carried out for different values of span length and bridge width. The optimum results for four different span lengths of 30, 40, 50, and 60 m with the deck width of 12 m are summarized in Table 6. As shown in Figure 8, optimum cost increases almost linearly with raising the span length, and for all of the span lengths the result of PSO is better than GA. Ascending curves in Figure 9 show that in order to obtain an optimum cost for a longer span, a higher concrete strength is required. In addition, by elongation of span length, depth and depth to span ratio of superstructure increase as shown in Figure 10 and 11. The amount of prestressing steel also increases almost linearly as shown in Figure 12. As it can be seen, the curves of PSO and GA are approximately similar in most of the cases which shows that there must be a meaningful relationship between span length and different variables.

The results of this optimization for four different bridge widths of 8, 10, 12, and 14 m with the span length of 50 m are summarized in Table 7. According to Figure 13, as the bridge width increases, optimum cost is nearly increased, and stronger concrete is generally picked up by the algorithms for wider deck (see Figure 14). The amount of prestressing steel also increases as shown in Figure 15. It is worth-mentioning that in Figures 13, the curves of PSO and GA are closely matched, while for all the bridge widths the optimum cost based on PSO is lower than GA.

Table 2. Optimum designs for different span lengths.

variable	unit	L=30		L=40		L=50		L=60	
		GA	PSO	GA	PSO	GA	PSO	GA	PSO
f_c'	MPa	37	36	37	43	40	48	43	50
h	m	1.68	1.69	2.45	2.33	3.19	3.21	3.81	3.92
T_t	cm	30	34	28	33	25	28	29	23
T_b	cm	21	21	20	19	20	19	20	19
T_w	cm	49	50	47	50	50	50	49	50
L_c	m	2.48	2.44	2.50	2.63	2.52	2.71	2.58	2.68
T_c	cm	23	20	25	26	22	24	24	19
T_s	cm	50	50	50	50	50	50	50	50
L_x	cm	157	160	170	158	149	140	152	160
L_y	cm	26	25	26	25	25	25	27	25
N_s	-	18	7	11	17	21	21	11	16
$N/2$	-	3	8	6	4	4	4	10	6
N_A	-	2	2	2	2	1	1	2	1
y_1	cm	40	23	24	49	51	56	100	37
η	%	76	75	76	76	77	76	82	78
ρ_σ	-	0.0096	0.0075	0.0118	0.0072	0.0138	0.0101	0.0101	0.0157
ρ_τ	-	0.0027	0.0026	0.0028	0.0029	0.0027	0.0029	0.0028	0.003
Cost	\$/m²	101.8	101.0	117.6	115.2	132.7	131.2	149.7	147.7

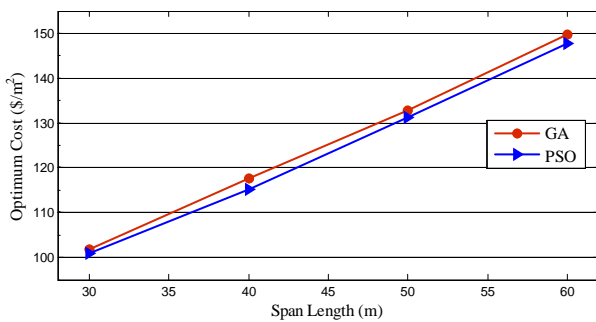


Fig. 8. Relation between optimum cost and span length.

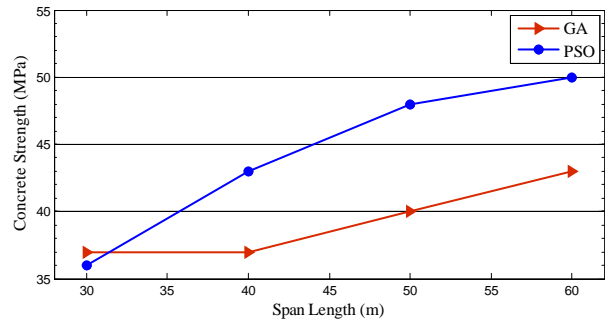


Fig. 9. Relation between concrete strength and length.

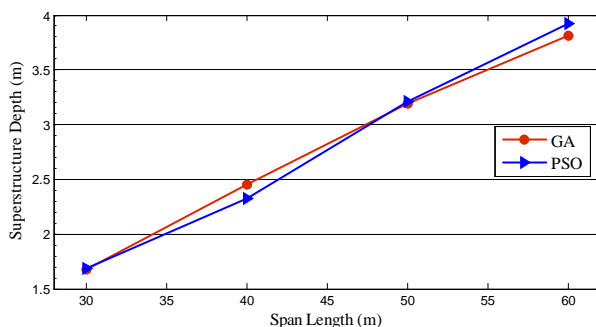


Fig. 10. Relation between depth and span length.

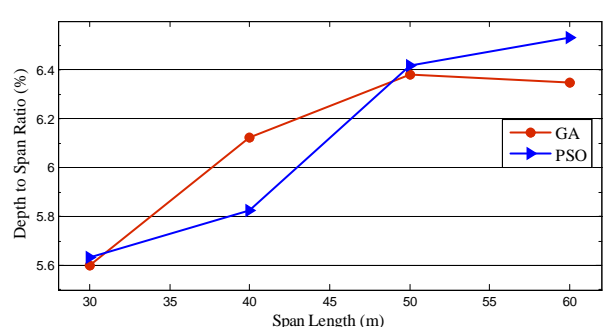


Fig. 11. Relation between depth to span ratio and length.

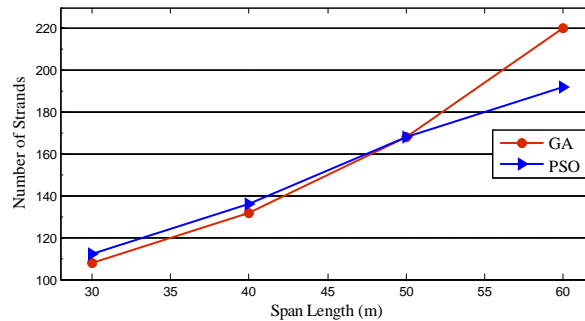


Fig. 12. Relation between prestressing steel and span length.

Table 3. Optimum designs for different bridge widths

variable	unit	W=8		W=10		W=12		W=14	
		GA	PSO	GA	PSO	GA	PSO	GA	PSO
f_c'	MPa	35	35	37	41	40	48	50	49
h	m	3.17	3.10	3.38	3.12	3.19	3.21	2.77	2.63
T_t	cm	27	30	26	29	25	28	30	35
T_b	cm	18	18	18	18	20	19	25	25
T_w	cm	39	38	45	45	50	50	48	50
L_c	m	1.98	2.00	2.44	2.50	2.52	2.71	2.79	2.77
T_c	cm	18	18	23	18	22	24	27	28
T_s	cm	43	43	49	50	50	50	50	50
L_x	cm	88	81	109	103	149	140	192	200
L_y	cm	26	25	27	27	25	25	25	25
N_s	-	18	14	21	13	21	21	19	18
$N/2$	-	3	4	3	5	4	4	6	7
N_A	-	1	1	1	1	1	1	2	2
y_1	cm	52	55	71	32	51	56	68	58
η	%	83	84	78	79	77	76	76	80
ρ_σ	-	0.0059	0.0047	0.0084	0.0065	0.0138	0.0101	0.0126	0.0092
ρ_τ	-	0.0029	0.0029	0.0027	0.0029	0.0027	0.0029	0.0039	0.0030
Cost	\$/m²	119.0	118.5	119.8	118.4	132.7	131.2	150.1	150.3

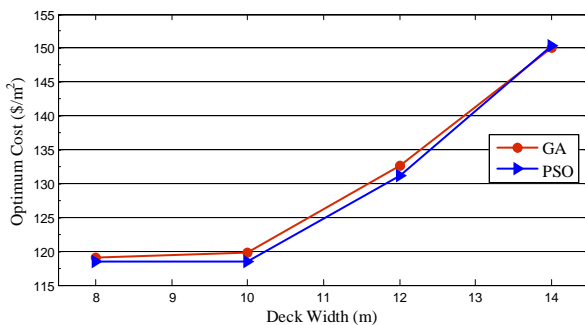


Fig. 13. Relation between concrete strength and width.

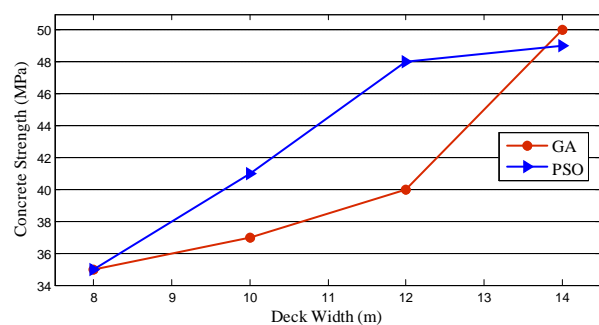


Fig. 14. Relation between optimum cost and width.

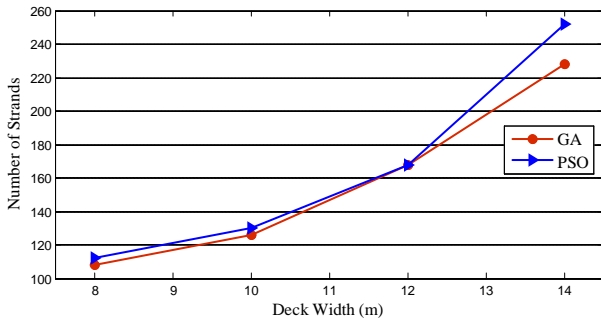


Fig. 15. Relation between prestressing steel and width.

Table 4. Optimum designs with different concrete unit costs for a bridge with the span length of 60 m and deck width of 12 m

Var.	unit	1C _c	2C _c	3C _c	4C _c	5C _c
<i>f_c'</i>	MPa	50	35	35	35	35
<i>h</i>	m	3.92	2.94	2.84	2.80	2.74
<i>T_t</i>	cm	23	30	27	25	23
<i>T_b</i>	cm	19	21	22	22	22
<i>T_w</i>	cm	50	50	35	36	33
<i>L_c</i>	m	2.68	2.38	2.39	2.40	2.39
<i>T_c</i>	cm	19	18	18	19	18
<i>T_s</i>	cm	50	50	50	50	50
<i>L_x</i>	cm	160	156	163	163	164
<i>L_y</i>	cm	25	25	25	25	25
<i>N_s</i>	-	16	15	22	22	18
<i>N_t/2</i>	-	6	6	4	4	5
<i>N_A</i>	-	1	2	1	2	2
<i>y₁</i>	cm	37	61	38	75	64
<i>η</i>	%	78	81	80	81	82
<i>ρ_σ</i>	-	0.0157	0.287	0.362	0.427	0.562
<i>ρ_x</i>	-	0.003	0.071	0.071	0.072	0.071
Cost	\$/m²	147.7	158.3	182.1	204.4	225.7

V. CONCLUSIONS

Cost optimum design of post-tensioned concrete box girder bridge superstructures is presented in this study. 17 different variables and a total of 140 constraints are considered based on AASHTO standard specifications and construction limitations. The objective function consists of material and construction costs involved in the bridge construction including concrete, prestressing steel, reinforcement, and formwork. Instead of using a lumped-sum value, all prestress losses are calculated by the code formulas for a greater precision. The Particle Swarm Optimization algorithm has been successfully used to solve the optimization problem, and in a short time an optimum design is obtained. In the bridge optimization problem with many variables and constraints, the viability of the PSO is demonstrated. The comparison between the PSO and the GA shows that the proposed PSO is more effective in finding an optimum solution.

Moreover, a parametric study is also conducted to investigate the effect of different values of span lengths and bridge widths on the optimum design. It is shown in the previous section that there is a meaningful relationship between span lengths of optimum bridges and some design variables. For instance, the depth of superstructure has an almost linear relation with span length, also concrete strength and number of strands increase with raising the bridge length. It is worth mentioning that the optimum cost linearly changes with the span length. Furthermore, cost, concrete strength, and number of strands increase as deck width of the bridge becomes larger. We have conducted this study based on specific design parameters and predetermined unit costs; however, it is possible to apply this optimization to a bridge with desired characteristics and unit costs.

REFERENCES

- [1] Hewson NR. Prestressed concrete bridges: design and construction: Thomas Telford; 2003.
- [2] Vanderplaats GN. Numerical optimization techniques for engineering design: with applications: McGraw-Hill New York; 1984.
- [3] Farshchin M, Camp CV, Maniat M. Optimal design of truss structures for size and shape with frequency constraints using a collaborative optimization strategy. Expert Systems with Applications. 2016 Dec 30;66:203-18.
- [4] Farshchin M, Camp CV, Maniat M. Multi-class teaching-learning-based optimization for truss design with frequency constraints. Engineering Structures. 2016 Jan 1;106:355-69.
- [5] Adeli H, Kamal O. Parallel Processing in Structural Engineering. London: Elsevier Applied Science; 1993.
- [6] Adeli H, Sarma KC. Cost optimization of structures: fuzzy logic, genetic algorithms, and parallel computing: John Wiley & Sons; 2006.
- [7] Sarma KC, Adeli H. Cost optimization of concrete structures. Journal of Structural Engineering. 1998;124:570-8.



ISSN: 2350-0328

International Journal of Advanced Research in Science, Engineering and Technology

Vol. 4, Issue 8 , August 2017

- [8] Hassanain MA, Loov RE. Cost optimization of concrete bridge infrastructure. *Canadian Journal of Civil Engineering*. 2003;30:841-9.
- [9] Fereig S. An application of linear programming to bridge design with standard prestressed girders. *Computers & structures*. 1994;50:455-69.
- [10] Fereig SM. Preliminary design of standard CPCI prestressed bridge girders by linear programming. *Canadian J. of Civil Eng.*1985;12:213-25.
- [11] Fereig SM. Preliminary design of precast prestressed concrete box girder bridges. *PCI Journal*. 1994;39:82-90.
- [12] Kirsch U. A bounding procedure for synthesis of prestressed systems. *Computers & structures*. 1985;20:885-95.
- [13] Goble G, Lapa W. Optimum design of prestressed beams. *ACI Journal Proceedings: ACI*; 1971.
- [14] Kirsch U. Optimum design of prestressed beams. *Computers & Structures*. 1972;2:573-83.
- [15] Naaman AE. Minimum cost versus minimum weight of prestressed slabs. *Journal of the Structural Division*. 1976;102:1493-505.
- [16] Cohn M, MacRae A. Optimization of structural concrete beams. *Journal of Structural Engineering*. 1984;110:1573-88.
- [17] Jones HL. Minimum cost prestressed concrete beam design. *Journal of Structural Engineering*. 1985;111:2464-78.
- [18] Cohn M, Lounis Z. Optimum limit design of continuous prestressed concrete beams. *Journal of Structural Engineering*. 1993;119:3551-70.
- [19] Torres GG-B, Brotchie J, Cornell C. a program for optimum design of prestressed concrete highway bridges. *journal prestressed concrete institute*. 1966;11:63-&.
- [20] Yu C, GUPTA ND, Paul H. Optimization of prestressed concrete bridge girders. *Engineering optimization*. 1986;10:13-24.
- [21] Barr A, Sarin S, Bishara A. procedure for structural optimization. *ACI Structural Journal*. 1989;86.
- [22] Lounis Z, Cohn MZ. Optimization of precast prestressed concrete bridge girder systems. *PCI J*. 1993;38:60-78.
- [23] Lounis Z, Cohn M. Computer-Aided Design of Prestressed Concrete Cellular Bridge Decks. *Computer-Aided Civil and Infrastructure Engineering*. 1995;10:1-11.
- [24] Lounis Z, Cohn M. An engineering approach to multicriteria optimization of bridge structures. *Computer-Aided Civil and Infrastructure Engineering*. 1995;10:233-8.
- [25] Lounis Z, Cohn M. An approach to preliminary design of precast pretensioned concrete bridge girders. *Computer-Aided Civil and Infrastructure Engineering*. 1996;11:381-93.
- [26] Fereig SM. Economic preliminary design of bridges with prestressed I-girders. *Journal of Bridge Engineering*. 1996;1:18-25.
- [27] Sirca Jr GF, Adeli H. Cost optimization of prestressed concrete bridges. *Journal of structural engineering*. 2005;131:380-8.
- [28] Aydin Z, Ayvaz Y. Optimum topology and shape design of prestressed concrete bridge girders using a genetic algorithm. *Structural and Multidisciplinary Optimization*. 2010;41:151-62.
- [29] Ahsan R, Rana S, Ghani SN. Cost Optimum Design of Posttensioned I-Girder Bridge Using Global Optimization Algorithm. *Journal of Structural Engineering*. 2011;138:273-84.
- [30] Kaveh, A., Maniat, M., & Naeini, M. A. (2016). Cost optimum design of post-tensioned concrete bridges using a modified colliding bodies optimization algorithm. *Advances in Engineering Software*, 98, 12-22.
- [31] Abbasi M, Zakeri B, Amiri GG. Probabilistic seismic assessment of multiframe concrete box-girder bridges with unequal-height piers. *Journal of Performance of Constructed Facilities*. 2015 Mar 3;30(2):04015016.
- [32] Abbasi M, Abedini MJ, Zakeri B, Ghodrati Amiri G. Seismic vulnerability assessment of a Californian multi-frame curved concrete box girder viaduct using fragility curves. *Structure and Infrastructure Engineering*. 2016 Dec 1;12(12):1585-601 .
- [33]Abbasi, M., and M.A. Moustafa. Effect of viscous damping modeling characteristics on seismic response of bridges. *Proceedings of Istanbul Bridge Conference, Istanbul, Turkey,8-10August, 2016 .*
- [34]Abbasi M, Moustafa MA. seismic fragility curves for system and individual components of multi-frame concrete box-girder bridges 2. 2017.
- [35] AASHTO. Standard Specifications for Highway Bridges. Washington, DC: American Association of State Highway and Transportation Officials; 2002.
- [36] Inc. F. The C Range post-tensioning system. 1999.
- [37] Eberhart RC, Kennedy J. A new optimizer using particle swarm theory. *Proceedings of the sixth international symposium on micro machine and human science: New York, NY; 1995. p. 39-43.*
- [38] Yang X-S. *Engineering optimization: an introduction with metaheuristic applications*: John Wiley & Sons; 2010.
- [39] Kaveh, A., and Maniat, M. (2015). Damage detection based on MCSS and PSO using modal data. *Smart Struct Syst*, 15(5), 1253-70.
- [40] Kaveh, A. and Maniat, M., (2014). Damage detection in skeletal structures based on charged system search optimization using incomplete modal data. *Int J Civil Eng IUST*, 12(2), pp.291-298.
- [41] Shi Y, Eberhart RC. Fuzzy adaptive particle swarm optimization. *Evolutionary Computation, 2001 Proceedings of the 2001 Congress on: IEEE; 2001. p. 101-6.*
- [42] Parsopoulos KE, Vrahatis MN. Parameter selection and adaptation in unified particle swarm optimization. *Mathematical and Computer Modelling*. 2007;46:198-213.
- [43] Arumugam MS, Rao M. On the improved performances of the particle swarm optimization algorithms with adaptive parameters, cross-over operators and root mean square (RMS) variants for computing optimal control of a class of hybrid systems. *Applied Soft Computing*. 2008;8:324-36.
- [44] Ratnaweera A, Halgamuge S, Watson HC. Self-organizing hierarchical particle swarm optimizer with time-varying acceleration coefficients. *Evolutionary Computation, IEEE Transactions on*. 2004;8:240-55.
- [45] Panigrahi B, Ravikumar Pandi V, Das S. Adaptive particle swarm optimization approach for static and dynamic economic load dispatch. *Energy conversion and management*. 2008;49:1407-15.
- [46] Nickabadi A, Ebadzadeh MM, Safabakhsh R. A novel particle swarm optimization algorithm with adaptive inertia weight. *Applied Soft Computing*. 2011;11:3658-70.